

Fluctuations of Apparent Entropy Production in Networks with Hidden Slow Degrees of Freedom

Matthias Uhl, Patrick Pietzonka and Udo Seifert

II. Institut für Theoretische Physik, Universität Stuttgart, 70550 Stuttgart, Germany

Abstract. The fluctuation theorem for entropy production is a remarkable symmetry of the distribution of produced entropy that holds universally in non-equilibrium steady states with Markovian dynamics. However, in systems with slow degrees of freedom that are hidden from the observer, it is not possible to infer the amount of produced entropy exactly. Previous work suggested that a relation similar to the fluctuation theorem may hold at least approximately for such systems if one considers an apparent entropy production. By extending the notion of apparent entropy production to discrete bipartite systems, we investigate which criteria have to be met for such a modified fluctuation theorem to hold in the large deviation limit. We use asymptotic approximations of the large deviation function to show that the probabilities of extreme events of apparent entropy production always obey a modified fluctuation theorem and, moreover, that it is possible to infer otherwise hidden properties. For the paradigmatic case of two coupled colloidal particles on rings the rate function of the apparent entropy production is calculated to illustrate this asymptotic behavior and to show that the modified fluctuation theorem observed experimentally for short observation times does not persist in the long time limit.

Keywords: Current fluctuations, Coarse-graining, Large deviation

1. Introduction

Stochastic thermodynamics has proven to be a reliable framework for the description of systems far from equilibrium. By extending the notion of classical thermodynamics to the level of single trajectories in a well defined way it allows us to identify laws from macroscopic thermodynamics like conservation of energy or the second law on the mesoscopic scale [1–3]. One important class of such relations are fluctuation theorems that constrain the probability distributions of fluctuating quantities like the work produced along a trajectory. A prominent example is the fluctuation theorem (FT) for the total entropy production in a non equilibrium steady state (NESS)

$$\ln \frac{p(\Delta s_{\text{tot}})}{p(-\Delta s_{\text{tot}})} = a \Delta s_{\text{tot}} \quad (1)$$

with $a = 1$, and we set $k_B = 1$ throughout this paper. It states that the probability of negative entropy production is exponentially suppressed and implies a positive average entropy production. It can therefore be seen as a refinement of the second law of thermodynamics to mesoscopic scales where fluctuations are still relevant.

For Markovian dynamics on a finite state space or finite dimensional driven Brownian diffusion, the FT follows as a mathematical identity, relying only on some rather technical conditions like existence and uniqueness of the stationary state. In addition, for a physical identification of the total entropy production, it is important that one has identified and taken into account all relevant slow degrees of freedom such that there is a clear time-scale separation between them and all other degrees of freedom. In this case the system evolves according to a Markovian dynamics described by a Langevin or Master equation.

This assumption is certainly fulfilled for the paradigmatic example of a Brownian particle in an aqueous solution serving as a heat bath, since it is safe to assume that collisions of the colloid with the molecules of the solvent happen on a different time-scale than the motion of the particle itself. However, the distinction between slow and fast degrees of freedom is often not that obvious, which has given rise to systematic studies of stochastic thermodynamics under an effective, coarse grained dynamics [4–12]. A fundamental problem in this context is the description of systems for which individual states are not discernible, so that an external observer can obtain only partial information about the trajectory in state space [13–15]. An understanding of these questions can lead to inference methods that allow the observer to reconstruct the hidden properties of the system [13, 16–19]. A recent study [20] emphasizes the conceptual similarities between a system with slow hidden degrees of freedom and a system coupled strongly to a heat bath [21, 22].

In the present paper we focus on systems with several slow degrees of freedom. The state space of such a system is the product space of the states of the individual degrees of freedom. Hence, if one of the degrees of freedom is deemed hidden from the observer [23–25], huge parts of this product space become indiscernible. We investigate the effects of such hidden slow degrees of freedom on the fluctuation theorem for entropy

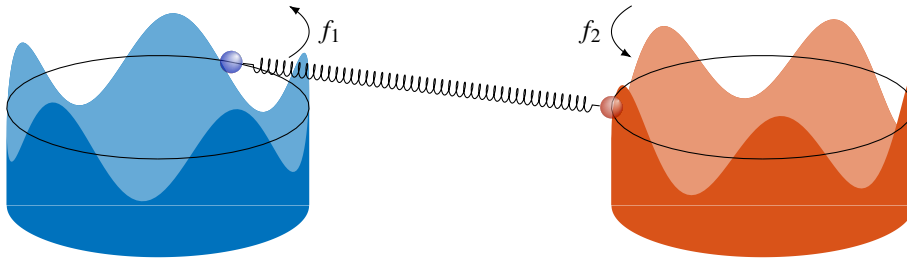


Figure 1. Two colloidal particles on rings coupled by an interaction force. If only one of the two is observable this setup serves as an example of a system with a slow hidden degree of freedom. Since the dynamics of the visible colloid is not Markovian the apparent entropy production of the visible part will in general not satisfy a FT.

production in the stationary state. More precisely, we use large deviation theory to analyze which conditions have to be met for a modified FT (1) with $a \neq 1$ to hold for the apparent entropy production obtained from an appropriate marginalization over slow hidden degrees of freedom in the limit of long observation times.

The experimental study performed by Mehl et al. [26] on a system of two coupled colloidal particles on rings, which could also be seen as a toy model for synchronization, see e.g. [27–29], has hinted at the approximate validity of the FT for a system consisting of two coupled colloidal particles on rings in aqueous solution that were each driven out of equilibrium by constant forces, as it is shown schematically in figure 1. While the combined system is still Markovian, the dynamics of an individual particle is not, since a time-scale separation is not valid for the two equally sized colloids. Naively inserting the visible dynamics into the definition of total entropy production in Markovian systems leads to an apparent entropy production, which was found to satisfy a modified FT (1) with $a \neq 1$ in a substantial range of parameters. However, this result can only be an approximation in some sense, since simulations of the system have revealed that there exist parameter combinations for which this relation does not hold and, hence, the right hand side of (1) is replaced by some non-linear antisymmetric function.

The aim of the present paper is to shed light on this behavior and to identify the criteria that have to be met for such a modified FT to hold. Since experimental data is by design limited to a finite number of experiments and large negative entropy production is rare, the modified FT has only been tested in a small region around zero in [26]. Therefore, these results could be explained simply by the fact that every antisymmetric function is linear around the origin. To overcome these limitations and to check whether similar results also hold in the long time limit and for untypical realizations of the apparent entropy production, we use a large deviation approach to this problem.

This paper is structured as follows. In section 2, we revisit the definitions used in [26] for systems with continuous degrees of freedom and define the apparent entropy production for a system with a discrete set of states. In section 3, we apply these definitions to a simple system with discrete states that is inspired by the one used in the

experiments. We identify parameter values for which the rate functions of the apparent entropy production approximately obeys a modified FT even when the observable and hidden degree of freedom are strongly coupled. The explanation of this behavior is presented in section 4, where we derive a bound on the rate function that becomes tight for large deviations from the mean and for which a modified FT holds. Based on an approximation to the characteristic polynomial of the so called tilted operator we show why in most cases the modified FT is not limited to the asymptotics of the rate function. In section 5, we calculate the rate function of systems of the type used by Mehl et al. in order to check whether our findings persist in the continuous limit. It turns out that the tails of the rate function still obey a modified FT exactly, while the deviations for smaller apparent entropy production rates are more pronounced than in the discrete case since the aforementioned approximation of the characteristic polynomial increasingly fails in the continuum limit case. Finally, we conclude in section 6.

2. Apparent Entropy Production

In systems with hidden degrees of freedom it is in general not possible to infer the total entropy production along a trajectory, since not all transitions are observable. In [26], the notion of an apparent entropy production was introduced that can be calculated from the observable dynamics and which is equivalent to the total entropy production if all slow degrees of freedom are observable.

In this section, we will shortly reproduce the definitions introduced in [26] for systems with continuous degrees of freedom and extend them to arbitrary discrete networks.

2.1. Continuous degrees of freedom

We assume that the time evolution of the probability density $p(\mathbf{x}, t)$ to find the system in state \mathbf{x} at time t is described by the Fokker-Planck equation

$$\partial_t p(\mathbf{x}, t) = -\nabla \mathbf{j}(\mathbf{x}, t) \quad (2)$$

with the probability current

$$\mathbf{j}(\mathbf{x}, t) \equiv \mu \mathbf{F}(\mathbf{x}) p(\mathbf{x}, t) - D \nabla p(\mathbf{x}, t), \quad (3)$$

where $\mathbf{F}(\mathbf{x})$ is the force acting on the system, D denotes the diffusivity, and $\mu = D/T$ is the mobility. From now on we use reduced units for time, space, energy, and temperature that allow us to set D , μ , and T to unity. The system will relax into a stationary state $p_s(\mathbf{x})$ for which the associated stationary current $\mathbf{j}_s(\mathbf{x})$ is divergence free. In a system with continuous degrees of freedom, the total entropy production up to time t can be calculated by integrating the product of the local mean velocity $\boldsymbol{\nu}(\mathbf{x}) \equiv \mathbf{j}_s(\mathbf{x})/p_s(\mathbf{x})$ with the fluctuating velocity along the trajectory,

$$\Delta S_{\text{tot}} = \int_0^t \boldsymbol{\nu}(\mathbf{x}(t')) \cdot \dot{\mathbf{x}}(t') dt' . \quad (4)$$

Now we assume that not all degrees of freedom are visible, i.e., the state \mathbf{x} is comprised of an observable part $\tilde{\mathbf{x}}$ and a hidden part $\hat{\mathbf{x}}$. Thus it is no longer possible to calculate the full mean velocity from observation of the visible degrees of freedom. Instead, only the observable components of the mean velocity $\tilde{\mathbf{v}}(\tilde{\mathbf{x}})$ conditioned on the visible state are accessible.

The apparent entropy is therefore defined in analogy to (4) as the integral

$$\Delta\tilde{s}_{\text{tot}} \equiv \int_0^t \tilde{\mathbf{v}}(\tilde{\mathbf{x}}(t')) \cdot \dot{\tilde{\mathbf{x}}}(t') dt' . \quad (5)$$

The visible mean velocity is related to the mean velocity of the full system through the marginalization

$$\tilde{\nu}_i(\tilde{\mathbf{x}}) \equiv \int \nu_i(\hat{\mathbf{x}}, \tilde{\mathbf{x}}) p_s(\hat{\mathbf{x}}|\tilde{\mathbf{x}}) d\hat{\mathbf{x}} , \quad (6)$$

where the index i is allowed to take values of the visible coordinates and $p_s(\hat{\mathbf{x}}|\tilde{\mathbf{x}})$ is the stationary probability to be in the hidden state $\hat{\mathbf{x}}$ provided the state $\tilde{\mathbf{x}}$ is observed.

2.2. Discrete Systems

In the same spirit it is possible to define the apparent entropy production if the system of interest is characterized by a discrete and finite set of states. As in the continuous case, we assume that each microstate is characterized by a visible label \tilde{n} and a hidden internal state \hat{n} . Microstates with the same visible label are grouped into mesostates. Transitions between the microstates take place with rates $w((\tilde{n}, \hat{n}) \rightarrow (\tilde{n}', \hat{n}'))$ and we denote the stationary distribution by $p_s(\tilde{n}, \hat{n})$. The observable stationary distribution of the visible states is given by

$$p_s(\tilde{n}) = \sum_{\hat{n}} p_s(\tilde{n}, \hat{n}) . \quad (7)$$

Due to the fact that not every transition is observable and that there is an ambiguity which transition takes place even if a transition is observed, it is in general impossible to determine the amount of produced entropy if one only observes a trajectory of the visible states. The only exception is a clear time-scale separation between the transitions within one mesostate and transitions between two different mesostates. In this case the dynamics can be described as a Markovian jump process on the level of the visible states and the total entropy production can be calculated as usual using the transition rates of this effective process.

Our main focus lies on the case where such a time-scale separation is not present. Even though the visible dynamics is not Markovian one can still define effective transition rates $\tilde{w}(\tilde{n} \rightarrow \tilde{n}')$ that describe how often a certain transition will occur on average per time unit provided that the system is initially in state \tilde{n} . For Markovian dynamics this definition would lead to the actual transition rates.

If the microscopic transition rates are known, the effective rates can be obtained by summation over all microscopic transitions that lead to a specific visible transition

$$\tilde{w}(\tilde{n} \rightarrow \tilde{n}') \equiv \frac{1}{p_s(\tilde{n})} \sum_{\hat{n}, \hat{n}'} w((\tilde{n}, \hat{n}) \rightarrow (\tilde{n}', \hat{n}')) p_s(\tilde{n}, \hat{n}). \quad (8)$$

These effective rates play the same role for the apparent entropy production in the discrete case as the mean velocity of the visible degree of freedom does in the continuous case. In the continuum limit, the mean velocity can indeed be obtained from the effective rates. In this limit, the effective rates are related to the local mean velocity conditioned on the visible state $\tilde{\nu}(\tilde{\mathbf{x}})$ in the same way as the microscopic rates are related to the unconditioned local mean velocity $\nu(\mathbf{x})$.

For discrete systems, the true entropy production along a trajectory is defined as [2]

$$\Delta S_{\text{tot}} = \sum_{n \rightarrow n'} \ln \frac{w(n \rightarrow n')}{w(n' \rightarrow n)} + \ln \frac{p_s(n_i)}{p_s(n_f)}, \quad (9)$$

where the sum runs over all jumps $n \rightarrow n'$ of the trajectory that begins in state n_i and ends in state n_f . If there are hidden degrees of freedom, we define the apparent entropy production by replacing all quantities in (9) with their observable counterparts, leading to

$$\Delta \tilde{S}_{\text{tot}} \equiv \sum_{\tilde{n} \rightarrow \tilde{n}'} \ln \frac{\tilde{w}(\tilde{n} \rightarrow \tilde{n}')}{\tilde{w}(\tilde{n}' \rightarrow \tilde{n})} + \ln \frac{p_s(\tilde{n}_i)}{p_s(\tilde{n}_f)}. \quad (10)$$

The long time limit of the distribution of apparent entropy production is captured by the rate function

$$h(u) = \lim_{t \rightarrow \infty} \frac{1}{t} \ln p(\Delta \tilde{S}_{\text{tot}} = ut, t). \quad (11)$$

Since the last term in (10) does not increase with time, it can be neglected for the calculation of the rate function.

We also assign a true affinity $\mathcal{A}_{\mathcal{C}}$ and an apparent affinity $\tilde{\mathcal{A}}_{\mathcal{C}}$ to every closed cycle \mathcal{C} in state space as the sum of all increments of true or apparent entropy production along the links of the cycle, i.e.

$$\mathcal{A}_{\mathcal{C}} \equiv \sum_{n \rightarrow n' \in \mathcal{C}} \ln \frac{w(n \rightarrow n')}{w(n' \rightarrow n)} \quad \text{and} \quad \tilde{\mathcal{A}}_{\mathcal{C}} \equiv \sum_{\tilde{n} \rightarrow \tilde{n}' \in \tilde{\mathcal{C}}} \ln \frac{\tilde{w}(\tilde{n} \rightarrow \tilde{n}')}{\tilde{w}(\tilde{n}' \rightarrow \tilde{n})}, \quad (12)$$

where $\tilde{\mathcal{C}}$ denotes the observable cycle corresponding to the cycle \mathcal{C} .

Even though the apparent entropy production is in general different from the true entropy production, we will nevertheless show that it approximately obeys a modified FT in the long time limit if certain conditions are met.

3. Bipartite lattice as a model system

3.1. General setup

We now present our system of interest. It consists of a two dimensional lattice of states (n_1, n_2) with N states in each dimension, as shown in figure 2. Transitions are possible

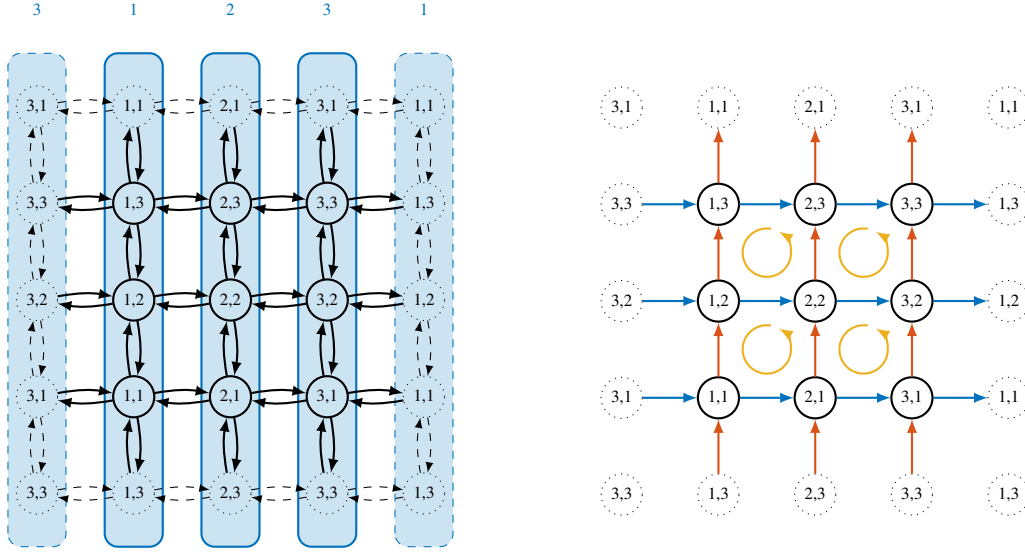


Figure 2. Visualization of the bipartite lattice for $N = 3$. Each state is labeled by a visible and a hidden coordinate. States with the same visible coordinate are grouped together into visible states. The graph on the right hand side shows the fundamental cycles of the network. These can be divided into three groups depending on their affinities and effective affinities.

between neighboring states with periodic boundary conditions. We assume that only the coordinate n_1 is visible and microstates within a column are indistinguishable for the observer.

Such a grid has $N^2 + 1$ fundamental cycles [30], which can be chosen as depicted in figure 2. As the colors indicate they can be split into three different categories. N of the cycles consist only of jumps that increase the visible coordinate. We therefore refer to them as visible cycles. In the same way there are also N hidden cycles that only have steps that increase the hidden coordinate. The other $(N - 1)^2$ are cycles that do not contain jumps across the periodic boundary conditions.

This system is, *inter alia*, inspired by the system of two coupled colloidal particles investigated in [26], where the system is driven out of equilibrium by two driving forces each acting on one colloid. To emulate this kind of driving in our discrete setup we demand that only cycles that correspond to a full rotation of a degree of freedom have a non vanishing affinity. Furthermore all affinities of the visible cycles should be equal to an affinity \mathcal{A}_1 and all affinities of the hidden cycles to another affinity \mathcal{A}_2 .

A set of rates meeting these conditions can be obtained by the ansatz of rates satisfying local detailed balance

$$w((n_1, n_2) \rightarrow (n_1 + 1, n_2)) = w_{n_1}^1 \exp((\mathcal{A}_1/N + V_{n_1, n_2} - V_{n_1+1, n_2})/2) \quad (13)$$

$$w((n_1 + 1, n_2) \rightarrow (n_1, n_2)) = w_{n_1}^1 \exp((-\mathcal{A}_1/N + V_{n_1+1, n_2} - V_{n_1, n_2})/2) \quad (14)$$

$$w((n_1, n_2) \rightarrow (n_1, n_2 + 1)) = w_{n_2}^2 \exp((\mathcal{A}_2/N + V_{n_1, n_2} - V_{n_1, n_2+1})/2) \quad (15)$$

$$w((n_1, n_2 + 1) \rightarrow (n_1, n_2)) = w_{n_2}^2 \exp((-\mathcal{A}_2/N + V_{n_1, n_2+1} - V_{n_1, n_2})/2), \quad (16)$$

where we introduce a potential energy V_{n_1, n_2} for each state and a characteristic timescale

w_n^i for each transition. This choice of rates ensures thermodynamic consistency and thus connects the physical properties of the system to its stochastic description [2]. If one chooses $w^i \propto N^2$ and the potential landscape as used in [26] as V , the discrete system becomes equivalent to the continuous system in the limit $N \rightarrow \infty$.

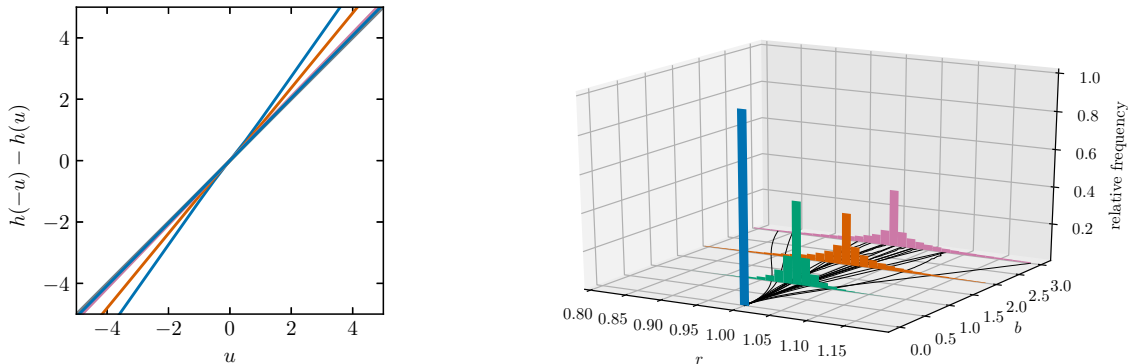


Figure 3. Fluctuation relations for ten randomly generated sets of rates (left) for parameters $\mathcal{A}_1 = \mathcal{A}_2 = b = 2$ and $N = 3$. In most cases the antisymmetric part of the generating function is approximately linear. This is also evident from the histograms on the right. They show the distribution of the ratio r (18) between slopes at zero and infinity of 10^5 randomly drawn sets of rates at different amplitudes of the coupling b . The curves on the bottom show this ratio for 20 different potential landscapes drawn from a Gaussian distribution with variance 1 that are scaled by the factor b .

3.2. Numerical results for random transition rates

We now present our first main result. For a small number of states the large deviation function for the apparent entropy production in a bipartite lattice obeys a modified FT for generic rates. Extensive numerical evidence shows that the antisymmetric part of the rate function typically does not deviate significantly from a linear behavior if the timescales w_n^i and the potential are drawn at random. The ensemble of random variations of the system is defined as follows: The potential energy V_{n_1, n_2} for each state is drawn from a Gaussian distribution with mean zero and standard deviation b . The timescales are chosen as

$$w_n^i = \exp(\psi_n^i - \bar{\psi}^i), \quad (17)$$

where the elements ψ_n^i are drawn from a uniform distribution between 0 and 2 and $\bar{\psi}^i \equiv \sum_n \psi_n^i / N$ denotes the average value of the elements. The rates drawn from this ensemble are then used to calculate first the effective rates for this system and then the rate function $h(u)$ of the apparent entropy production (for details on the procedure see section 4.1). A few representative results of the antisymmetric part of the rate function $h(-u) - h(u)$ for $N = 3$ are shown on the left panel of figure 3. They are evidently linear, which means that a modified FT is valid for the distribution of apparent entropy production in these cases. To affirm this finding with better statistics we perform this

calculation repeatedly for different values of b and check the result for linearity. This is done by calculating the ratio

$$r \equiv a_0/a_\infty \quad (18)$$

of the slope at $u = 0$, $a_0 \equiv -2h'(0)$, and the asymptotic slope $a_\infty \equiv \lim_{u \rightarrow \infty} (h(-u) - h(u))/u$. The latter is well defined and can be calculated directly from the (effective) rates as will be explained in section 4.

The right panel of figure 3 shows histograms of the quantity r demonstrating the approximate validity of an FT for different coupling strengths calculated from 10^5 numerical experiments for each different value of b . The affinities of the observable and hidden cycles were chosen as $\mathcal{A}_1 = \mathcal{A}_2 = 1$. If there is no potential present ($b = 0$), the ratio is exactly 1 and the antisymmetric part of the rate function is linear in all cases since the two degrees of freedom are independent and the effective rates are identical to the jump rates of the visible degree of freedom. Interestingly, this behavior changes only little even if the coupling becomes strong. For example, in the case $b = 3$, the average potential difference of one jump alone exceeds the affinity of one full rotation of a degree of freedom but nevertheless a modified FT is still valid for this parameter combination in most cases.

4. Bounds and approximations

The numerical results for the rate function for apparent entropy production in the previous section have shown that a modified FT generically holds in very good approximation. In this section we will focus on the underlying structure that leads to this behavior.

4.1. Large deviations of integrated currents

First we introduce the elements from large deviation theory needed for the scope of our calculations. For a more complete introduction, see, e.g., [31].

The quantities of interest in this paper are distributions of integrated currents. In a stochastic system with discrete states $\{n\}$ integrated currents are functionals of the trajectory $n(t')$ where we assign an increment $d_{n,n'} = -d_{n',n}$ to each transition $n \rightarrow n'$ and sum over all transitions that have occurred

$$X[n(\cdot)] = \sum_{n \rightarrow n'} d_{n,n'}. \quad (19)$$

In the continuous limit this sum becomes an integral along the trajectory

$$X[\mathbf{x}(\cdot)] = \int_0^t \mathbf{d}(\mathbf{x}(t')) \cdot \dot{\mathbf{x}}(t') dt'. \quad (20)$$

The apparent entropy production is an integrated current with the choice $d_{\tilde{n},\tilde{n}'} = \ln \tilde{w}(\tilde{n} \rightarrow \tilde{n}')/\tilde{w}(\tilde{n}' \rightarrow \tilde{n})$ in the discrete and $\mathbf{d}(\mathbf{x}) = \tilde{\nu}(\mathbf{x})$ in the continuous case.

The results derived in this paper are essentially relations and statements about the long time behavior of the probability distributions $p(X, t)$ of integrated currents. It can

be shown that for long enough times these probabilities will decay exponentially, thus motivating the definition of a rate function [31]

$$h(u) \equiv - \lim_{t \rightarrow \infty} \frac{1}{t} p(X = ut, t) \quad (21)$$

that characterizes the speed of this decay.

The rate function can be obtained without the explicit knowledge of the distribution through Legendre-Fenchel-transformation of the rescaled cumulant generating function

$$\alpha(\lambda) \equiv \lim_{t \rightarrow \infty} \frac{1}{t} \ln \langle e^{\lambda X} \rangle \quad (22)$$

as

$$h(u) = \sup_{\lambda} [u\lambda - \alpha(\lambda)] . \quad (23)$$

In general, the generating function can be obtained by determining the time evolution of the moment generating function conditioned on the final state of the trajectory

$$g(\lambda, \mathbf{x}, t) \equiv \langle e^{\lambda X} \rangle_{\mathbf{x}} , \quad (24)$$

where the possibly discrete index \mathbf{x} indicates that for the expectation value only those trajectories are taken into account that end in state \mathbf{x} . This time evolution is generated by the so called tilted master operator $\mathcal{L}(\lambda)$ leading to

$$\partial_t g(\lambda, \mathbf{x}, t) = \mathcal{L}(\lambda) g(\lambda, \mathbf{x}, t) . \quad (25)$$

In the case of an integrated current defined on a discrete set of states as in (19) the explicit form of $\mathcal{L}(\lambda)$ reads

$$\mathcal{L}(\lambda) = w(n \rightarrow n') \exp(d_{n',n}\lambda) - \delta_{n,n'} \sum_{n'} w(n \rightarrow n') . \quad (26)$$

It can be shown that the generating function $\alpha(\lambda)$ is the Perron-Frobenius eigenvalue of the tilted operator $\mathcal{L}(\lambda)$. We can therefore calculate the rate function by diagonalizing this operator and performing a Legendre-Fenchel-transformation of the eigenvalue with the largest real part.

This paper is concerned with the question whether the distribution of certain integrated currents obey a FT of the form $\ln(p(X, t)/p(-X, t)) = \lambda_0 X$ in the long time limit, where λ_0 corresponds to the slope a of the modified FT (1). In terms of the rate function and the generating function, such a relation is expressed by the two equivalent relations

$$\alpha(\lambda) = \alpha(-\lambda_0 - \lambda) \quad \Leftrightarrow \quad h(-u) - h(u) = \lambda_0 u . \quad (27)$$

In words, the rate function obeys a modified FT if and only if the generating function is symmetric around a value corresponding to the negative slope appearing in the FT.

One important aspect to note at this point is that since we know that $\alpha(\lambda)$ is convex, the Legendre-Fenchel-Transformation is a one to one mapping between individual points of the two functions. Therefore (27) is also valid locally in the sense that, if there exists some, not necessarily connected, region in the λ domain in which the left hand side of (27) holds, there must also exist a region in u where the right hand side holds.

4.2. Asymptotic behavior of the rate function

In previous work [32], it was shown that the generating function of any integrated current in a discrete network will approach an exponential function from above as its argument goes to infinity. For the present problem this asymptotic bound can be constructed as follows. If we choose an arbitrary closed path \mathcal{C} on the network with length $N_{\mathcal{C}}$, which we denote as

$$\mathcal{C} \equiv [n(1) \rightarrow n(2) \rightarrow \dots \rightarrow n(N_{\mathcal{C}}) \rightarrow n(1)] , \quad (28)$$

we can assign to it the geometric mean of transition rates along the path

$$\gamma_{\mathcal{C}} \equiv \left(\prod_{i=1}^{N_{\mathcal{C}}-1} w(n(i) \rightarrow n(i+1)) \right)^{1/N_{\mathcal{C}}} \quad (29)$$

as well as the number $\mathbf{n}_{\mathcal{C}}$ of visible cycles completed by the path \mathcal{C} . It was shown in [32] that each path implies a lower bound on the generating function for the apparent entropy production of the form

$$\alpha(\lambda) \geq f(\lambda, \mathcal{C}) \equiv \gamma_{\mathcal{C}} \exp \left(\frac{\mathbf{n}_{\mathcal{C}}}{N_{\mathcal{C}}} \tilde{\mathcal{A}} \lambda \right) - \max_n r_n , \quad (30)$$

where $\tilde{\mathcal{A}}$ is the apparent affinity from (12) of the unique cycle in the visible state space, and where r_n denotes the exit rate of the state n .

For large λ , the strongest bound is achieved by the path \mathcal{C}_+ that has the largest ratio of completed visible cycles $\mathbf{n}_{\mathcal{C}}$ to number of jumps $N_{\mathcal{C}}$. Obviously this is a cycle that only jumps in positive n_1 direction while maintaining the state of the hidden degree of freedom (shown in blue in figure 2), since any additional step in the hidden direction would increase the length of the cycle while maintaining the same winding number and would therefore lead to a lower ratio. Among those cycles the one with the highest geometric mean of the rates leads to the strongest bound.

For $\lambda \rightarrow -\infty$ the optimal cycle is the same one but traversed in opposite direction. We denote this path by \mathcal{C}_- . The bound induced by \mathcal{C}_- is related to the one induced by \mathcal{C}_+ through the relation

$$f(\lambda, \mathcal{C}_-) = f \left(-\frac{\mathcal{A}_1}{\tilde{\mathcal{A}}} - \lambda, \mathcal{C}_+ \right) , \quad (31)$$

as can be shown using the relation of the geometric mean in forward and backward direction with the affinity of a visible cycle

$$\frac{\gamma_{\mathcal{C}_+}}{\gamma_{\mathcal{C}_-}} = \exp \left(\frac{\mathcal{A}_1}{N_{\mathcal{C}}} \right) . \quad (32)$$

The numerical evidence presented in [32] indicates that this bound becomes tight in the limit $\lambda \rightarrow \pm\infty$ in the sense that the ratio of the generating function and the bound converges to 1. As a consequence, (31) implies that the tails of the generating function are symmetric around $\lambda = -\mathcal{A}_1/(2\tilde{\mathcal{A}})$. Following (27) the rate function hence obeys a modified FT of the form

$$h(-u) - h(u) = \frac{\mathcal{A}_1}{\tilde{\mathcal{A}}} u \quad (33)$$

asymptotically for large $|u|$.

This relation also shows that, in principle, it is possible to infer the amount of true entropy produced in one rotation of the visible degree of freedom from the statistics of the extremes of the apparent entropy production, since these are generated by trajectories for which the hidden degree of freedom is not changing. The only knowledge about the system that is a priori necessary for such an inference is that the visible degree of freedom has indeed a cyclic structure, with which the affinity \mathcal{A}_1 can be associated, and that the coupling strength to the hidden degree of freedom is finite. Further knowledge, e.g. about the transition rates or the number of visible and hidden states, is not required.

4.3. Symmetric approximation of the generating function

The numerical evidence presented in section 3 indicates that the linear behavior of the antisymmetric part of the rate function is not limited to the extremes of the distribution but is also present for smaller arguments of the rate function. The goal of this section is to derive a symmetric approximation on the characteristic polynomial of the tilted master operator defined as

$$\chi(\lambda, y) \equiv \det(\mathcal{L}(\lambda) - y) = \sum_{\pi \in S_{N^2}} \text{sgn}(\pi) \prod_n [\mathcal{L}_{n, \pi(n)}(\lambda) - y \delta_{n, \pi(n)}] , \quad (34)$$

where the sum runs over the set S_{N^2} of all possible permutations π of state space. Since the generating function is the largest eigenvalue of $\mathcal{L}(\lambda)$ and hence the largest root of $\chi(\lambda, y)$ in y for any given value of λ , the validity of such an approximation would imply a modified FT.

Because the fundamental cycles of the bipartite grid split into three categories depending on their combination of effective and actual affinity as described in section 3, the sum over permutations can be expressed in the form (see appendix)

$$\chi(\lambda, y) = \sum_{\pi \in S_{N^2}} \text{sgn}(\pi) f_{\pi}(y) \cosh \left[\mathbf{n}_{\pi} \left(\tilde{\mathcal{A}}\lambda + \mathcal{A}_1/2 \right) + \mathbf{m}_{\pi} \mathcal{A}_2/2 \right] . \quad (35)$$

The two integers \mathbf{n}_{π} and \mathbf{m}_{π} are winding numbers that count how often the permutation links states across the periodic boundary condition in the positive observable and hidden direction respectively. The polynomial $f_{\pi}(y)$ is the only part of each term that depends on y and its degree is bounded from above by $N^2 - N(|\mathbf{n}_{\pi}| + |\mathbf{m}_{\pi}|)$.

A symmetric approximation to the characteristic polynomial

$$\chi^{\text{sym}}(\lambda, y) \equiv \sum_{\pi \in S_{N^2} | \mathbf{n}_{\pi} \cdot \mathbf{m}_{\pi} = 0} \text{sgn}(\pi) f_{\pi}(y) \cosh \left[\mathbf{n}_{\pi} \left(\tilde{\mathcal{A}}\lambda + \mathcal{A}_1/2 \right) + \mathbf{m}_{\pi} \mathcal{A}_2/2 \right] \quad (36)$$

with the same center of symmetry as the asymptotes of the generating function can now be constructed by summing only over those terms where either the visible, \mathbf{n}_{π} or the hidden winding number \mathbf{m}_{π} vanishes. That this procedure tends to be a good approximation at least for a low number of states N can be understood simply by counting the remaining non-vanishing terms by their combination of winding numbers.

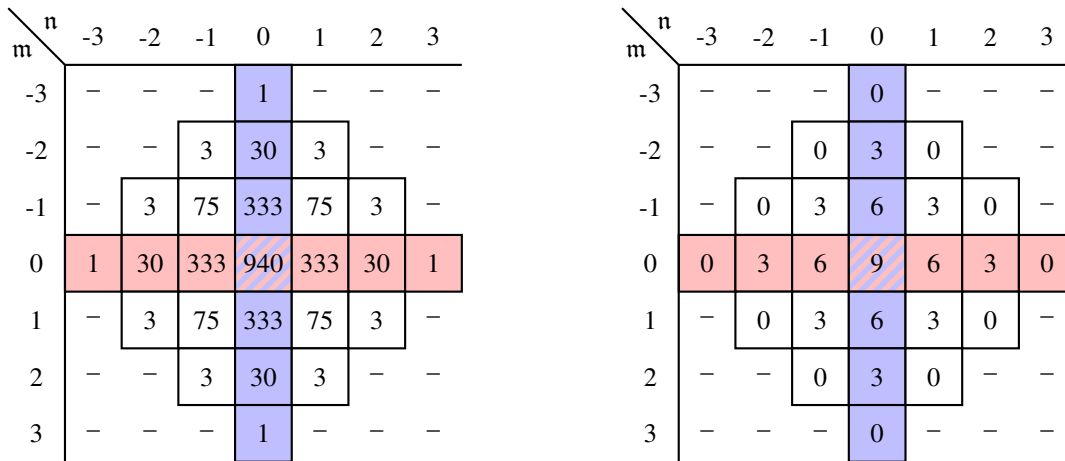


Figure 4. Left: number of permutations with a specific combination of winding numbers for $N = 3$. For most permutations either the visible winding number (blue) or the hidden winding number (red) vanishes. Right: The table shows the highest possible degree of the polynomial $f_\pi(y)$ corresponding to a permutation with given winding numbers \mathbf{n}_π and \mathbf{m}_π . It is evident permutations with $\mathbf{n}_\pi \cdot \mathbf{m}_\pi \neq 0$ do not depend as strongly on y as most other permutations.

The result is shown for $N = 3$ in figure 4. It turns out that skipping terms with $\mathbf{n}_\pi \cdot \mathbf{m}_\pi \neq 0$ omits only 324 of a total of 3720 terms.

Furthermore it can be argued that terms with $\mathbf{n}_\pi \cdot \mathbf{m}_\pi \neq 0$ will not depend as strongly on y and are therefore less significant for the position of the roots. The only part of the term depending on y is the polynomial $f_\pi(y)$, whose degree is coupled to the winding numbers. The highest possible degree of $f_\pi(y)$ is listed in the right panel of figure 4 depending on the values of the two winding numbers.

An example for a typical characteristic polynomial and the corresponding symmetric approximation is shown in figure 5. It is evident that this approximation not only captures the behavior of the largest eigenvalue but also describes the behavior of the subdominant eigenvalues quite well.

4.4. Deviations from the fluctuation theorem

While the omission of terms in the characteristic polynomial that are not symmetric under the replacement $\lambda \rightarrow -\mathcal{A}_1/\tilde{\mathcal{A}} - \lambda$ leads to an approximation that works rather well in most cases, we can also identify those rare cases where the generating function is pronouncedly asymmetric. In these instances terms with $\mathbf{n}_\pi \cdot \mathbf{m}_\pi \neq 0$ must make a significant contribution to the characteristic polynomial. This happens if the rates are large along a cyclic path for which both winding numbers do not vanish. Moreover, rates that lead away from this path have to be small while rates pointing towards the path are large. These conditions are met for example if we choose the potential as

$$V_{n_1, n_2} = V_0 \begin{pmatrix} 0 & 0 & 1 \\ 1 & 0 & 0 \\ 0 & 1 & 0 \end{pmatrix}. \quad (37)$$

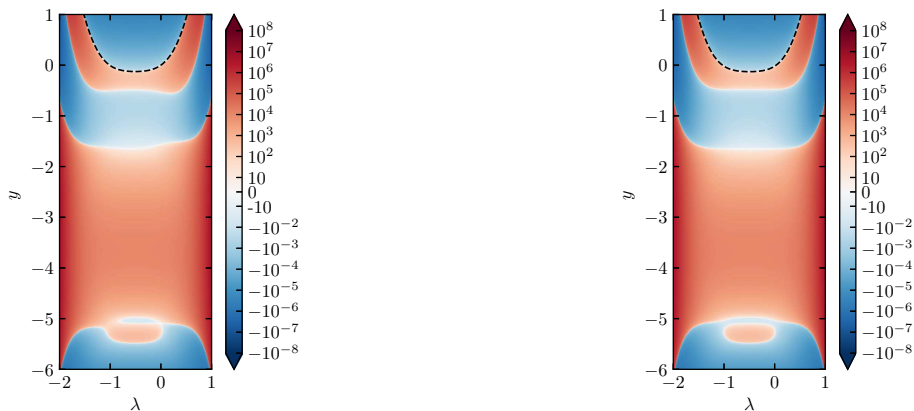


Figure 5. Logarithmic plot of the characteristic polynomial $\chi(\lambda, y)$ (left) and the symmetric approximation $\chi^{\text{sym}}(\lambda, y)$ (right) obtained by only summing over terms with at least one vanishing winding number. This is a good approximation in the region where the largest eigenvalue (indicated as dashed line) lies, which explains the approximate symmetry of the generating function.

If V_0 is sufficiently large, this potential will force the system to jump only between states with vanishing potential while jumps onto the potential barriers are suppressed.

As a result of the lack of symmetry in the generating function, the antisymmetric part of the rate function shows a pronounced non-linear behavior for small values of $|u|$ while it still approaches an asymptotic slope for large $|u|$ as a consequence of the asymptotic relation (33). This is shown in figure 6 where the affinities of the two degrees of freedom were chosen to be equal.

In this specific case the system will most likely perform an asymmetric random walk along the potential “valley”. For this kind of dynamics, the generating function $\alpha_{\text{RW}}(\lambda)$ and the rate function $h_{\text{RW}}(u)$ for the total entropy production are known and obey the usual Gallavotti-Cohen-symmetry [33] and the FT. Since we are considering not the total but the apparent entropy production these results have to be rescaled by the ratio of the total entropy production to the apparent entropy production per rotation, i.e.

$$\alpha(\lambda) = \alpha_{\text{RW}} \left(\frac{\tilde{\mathcal{A}}}{\mathcal{A}_1 + \mathcal{A}_2} \lambda \right) \quad (38)$$

$$h(u) = h_{\text{RW}} \left(\frac{\mathcal{A}_1 + \mathcal{A}_2}{\tilde{\mathcal{A}}} u \right). \quad (39)$$

We therefore expect the rate function to obey a modified FT with slope $(\mathcal{A}_1 + \mathcal{A}_2)/\tilde{\mathcal{A}}$ for small $|u|$ if the potential barriers are large as shown in figure 6.

On the other hand the asymptotic bound is determined by those periodic trajectories that minimize the apparent entropy production per jump. Clearly those are the trajectories that always jump in one direction along the visible axis. They produce \mathcal{A}_1 of total entropy per turn, which leads with the same arguments as above to the slope $\mathcal{A}_1/\tilde{\mathcal{A}}$.

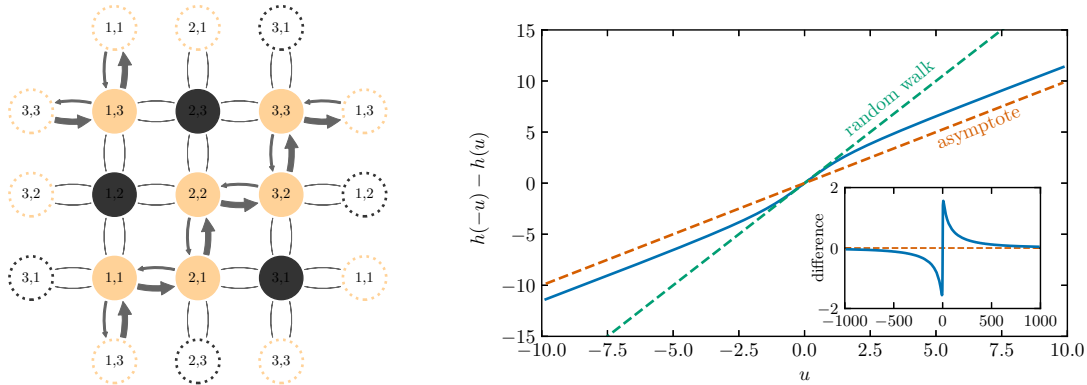


Figure 6. Stationary distribution and antisymmetric part of the rate function for a network with rates designed to break the modified FT. The states are colored according to their respective stationary distribution (lighter means higher p_s). The width of the arrows are scaled by the likelihood of observing a specific transition $w(\mathbf{n} \rightarrow \mathbf{n}')p_s(\mathbf{n})$. The affinities were set to $\mathcal{A}_1 = \mathcal{A}_2 = 3$ and the height of the potential barrier to $V_0 = 10$. The antisymmetric part of the rate function shows a pronounced non-linear behavior close to the origin and reaches a linear asymptote. The inset shows the difference to the asymptote over a larger interval of u . The slope at the origin is described by the appropriately rescaled FT for the asymmetric random walk.

5. Continuous case

So far, we have explained the generic emergence of a modified FT for the bipartite lattice. Transferring this result to a system with continuous degrees of freedom governed by a Langevin equation like the one used in [26] is not trivial. First, the asymptotic bound used in the previous section to derive the asymptotic slope of the asymmetric part of the rate function is not valid for continuous systems since the limit $\lambda \rightarrow \infty$ does not commute with the limit $N \rightarrow \infty$. When the number of states increases, the region in which the asymptotic bound is a good approximation moves outwards leading to quadratic (rather than exponential) tails of the generating function in the case of a continuous state space.

5.1. Asymptotic bound

In this section, we will derive a bound on the generating function similar to the auxiliary bound introduced in [34] for a one dimensional system that will become tight up to a constant for large $|\lambda|$ and is also symmetric. It can therefore replace the asymptotic bound in the derivation of the asymptotic slope of the antisymmetric part of the rate function. Interestingly, it will turn out that the center of symmetry of this new bound is the same as for the one used in the discrete case. This means that the asymptotic slope survives the continuum limit despite the fact that the bound which it was originally based on does not.

We consider two dimensional dynamics governed by the coupled Langevin equations

$$\dot{x}_1(t) = f_1 - \partial_{x_1} V(x_1, x_2) + \xi_1(t) \quad (40)$$

$$\dot{x}_2(t) = f_2 - \partial_{x_2} V(x_1, x_2) + \xi_2(t) \quad (41)$$

with periodic boundary conditions identifying x_i and $x_i + 2\pi$ and the random forces $\xi_i(t)$ with

$$\langle \xi_i(t) \xi_j(t') \rangle = 2\delta_{i,j} \delta(t - t'). \quad (42)$$

In the long time limit, the apparent entropy production depends only on the distance Δx_1 traveled by the first degree of freedom, since

$$\Delta \tilde{s}_{\text{tot}} = \int_0^t \tilde{\nu}_1(x_1) \dot{x}_1(t') dt' \approx \frac{\tilde{\mathcal{A}}}{2\pi} \Delta x_1 \quad \text{with} \quad \tilde{\mathcal{A}} \equiv \int_0^{2\pi} \tilde{\nu}_1(x_1) dx_1. \quad (43)$$

up to finite boundary terms. Therefore, we calculate first the generating function for the distance Δx , which we denote by $\alpha_x(\lambda_x)$, and obtain the generating function for $\Delta \tilde{s}_{\text{tot}}$ through rescaling of this function. We use the index x to distinguish the respective functions and arguments for the traveled distance from the ones for apparent entropy production. The tilted operator for the distance was derived in [35] and for a more general case in [36] and is given by

$$\mathcal{L}(\lambda_x) = \mathcal{L}_0 + \mathcal{L}_1 \lambda_x + \lambda_x^2 \quad (44)$$

where \mathcal{L}_0 denotes the Fokker-Planck operator

$$\mathcal{L}_0 = \sum_{i \in \{1,2\}} -\partial_{x_i} [F_i(\mathbf{x}) - \partial_{x_i}] \quad (45)$$

and

$$\mathcal{L}_1 = F_1(\mathbf{x}) - 2\partial_{x_1}. \quad (46)$$

From this form of the tilted operator it is obvious that its largest eigenvalue, the generating function, does not increase exponentially but quadratically $\alpha_x(\lambda_x) = \lambda_x^2 + \mathcal{O}(\lambda_x)$.

In order to show that the generating function becomes symmetric, we use the general result from [37] (see also [38, 39]) for the rate function for the probability to observe a given empirical distribution

$$\varrho(\mathbf{x}) \equiv \frac{1}{t} \int_0^t \delta(\mathbf{x}(t') - \mathbf{x}) dt' \quad (47)$$

and empirical currents

$$\boldsymbol{\mu}(\mathbf{x}) \equiv \frac{1}{t} \int_0^t \dot{\mathbf{x}}(t') \delta(\mathbf{x}(t') - \mathbf{x}) dt' \quad (48)$$

that is given by

$$I[\varrho(\cdot), \boldsymbol{\mu}(\cdot)] = \frac{1}{4} \int d\mathbf{x} \varrho(\mathbf{x}) \left[\frac{\boldsymbol{\mu}(\mathbf{x}) - \mathbf{j}_\varrho(\mathbf{x})}{\varrho(\mathbf{x})} \right]^2. \quad (49)$$

Here $\mathbf{j}_\varrho(\mathbf{x})$ denotes the probability current according to (3) if the distribution $p(\mathbf{x}, t)$ is replaced by the empirical distribution $\varrho(\mathbf{x})$. Since the empirical current uniquely determines Δx_1 , it is in principle possible to calculate the rate function $h_x(u_x)$ by the contraction principle, as

$$h_x(u_x) = \min_{\varrho(\mathbf{x})} \min_{\boldsymbol{\mu}(\mathbf{x})|u_x[\boldsymbol{\mu}]=u_x} I[\varrho(\mathbf{x}), \boldsymbol{\mu}(\mathbf{x})], \quad (50)$$

where the minimization runs over all functions $\varrho(\mathbf{x})$ and $\boldsymbol{\mu}(\mathbf{x})$ fulfilling the additional constraint $\nabla \boldsymbol{\mu}(\mathbf{x}) = 0$ that lead to the desired value of the integrated current. Although this minimization is not feasible for most systems, we can obtain an upper bound on the rate function if we insert a suitable ansatz and minimize with respect to the parameters therein.

For our purpose it is sufficient to insert the arguably simplest form of empirical distribution and current, the constant functions

$$\varrho(\mathbf{x}) = \frac{1}{4\pi^2} \quad \text{and} \quad \boldsymbol{\mu}(\mathbf{x}) = \frac{1}{4\pi^2} (\mu_1 \mathbf{e}_1 + \mu_2 \mathbf{e}_2). \quad (51)$$

To get a bound on the rate function for the apparent entropy production we have to minimize I with respect to the free parameters μ_1 and μ_2 subject to the condition that the empirical current reproduces the desired value of u_x . This procedure fixes μ_1 , since

$$u_x = \frac{\Delta x_1}{t} = \frac{1}{4\pi^2} \int \mu_1 d\mathbf{x} = \mu_1, \quad (52)$$

leaving us with

$$\begin{aligned} I[\varrho(\mathbf{x}), \boldsymbol{\mu}(\mathbf{x})] &= \frac{1}{4} \int d\mathbf{x} \frac{1}{4\pi^2} [(u_x - f_1)^2 + 2(u_x - f_1)(\partial_{x_1} V(\mathbf{x})) + (\partial_{x_1} V(\mathbf{x}))^2 \\ &\quad + (\mu_2 - f_2)^2 + 2(\mu_2 - f_2)(\partial_{x_2} V(\mathbf{x})) + (\partial_{x_2} V(\mathbf{x}))^2] \\ &= \frac{1}{4} \left[(u_x - f_1)^2 + \overline{(\partial_{x_1} V)^2} + \overline{(\partial_{x_2} V)^2} \right] + (\mu_2 - f_2)^2 / 4, \end{aligned} \quad (53)$$

where we use the notation $\overline{A(\mathbf{x})} \equiv \int A(\mathbf{x}) d\mathbf{x} / (4\pi^2)$ to denote the average value of a function. This relation reaches a minimum if the last term vanishes. Minimization thus yields the upper bound on the rate function

$$h_x(u_x) \leq \min_{\mu_2} I[\varrho(\mathbf{x}), \boldsymbol{\mu}(\mathbf{x})] = \frac{1}{4} \left[(u_x - f_1)^2 + \overline{(\partial_{x_1} V)^2} + \overline{(\partial_{x_2} V)^2} \right] \quad (54)$$

corresponding to a lower bound on the generating function

$$\alpha_x(\lambda_x) = \max_{u_x} [u_x \lambda_x - h_x(u_x)] \geq (\lambda_x + f_1) \lambda_x - \frac{1}{4} \left[\overline{(\partial_{x_1} V)^2} + \overline{(\partial_{x_2} V)^2} \right]. \quad (55)$$

Since the bound and the generating function behave for large arguments like a quadratic function with the same curvature and since they must not intersect, the bound can asymptotically differ only by a constant from the generating function

$$\alpha_x(\lambda_x) = (\lambda_x + f_1) \lambda_x + \mathcal{O}(1). \quad (56)$$

Following the same arguments as in the discrete case, this scaling corresponds to a asymptotic linear behavior of the antisymmetric part of the rate function.

$$h_x(-u_x) - h_x(u_x) \sim f_1 u_x. \quad (57)$$

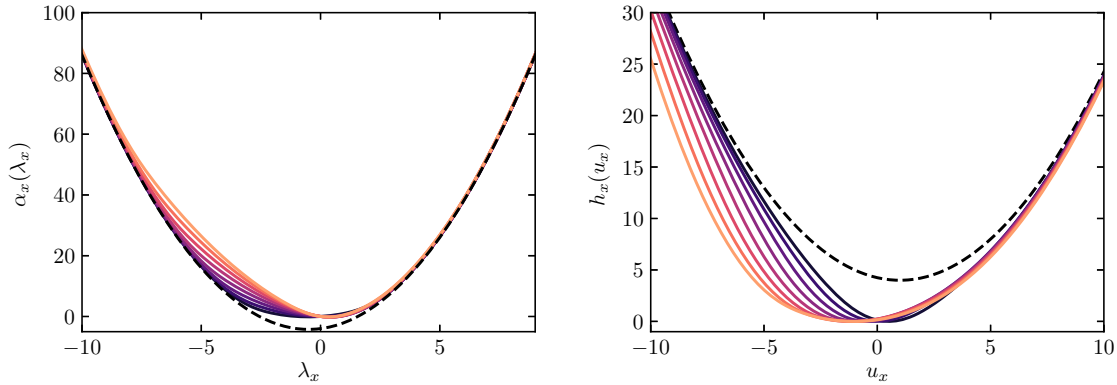


Figure 7. Generating function $\alpha_x(\lambda_x)$ and rate function $h_x(u_x)$ for the two ring system with coupling potential $V = 4 \cos(x_1 + x_2)$. The force on the visible degree of freedom is fixed at $f_1 = 1$, the force on the hidden degree of freedom varies from $f_2 = 0$ (dark) to $f_2 = 7$ (light).

If we use the rescaling between the traveled distance and the apparent entropy production $u_x = 2\pi u / \tilde{\mathcal{A}}$, this relation is equivalent to the one found for discrete systems in (33).

5.2. Numerical case study

While this expression shows that the asymptotics of the rate function obeys a modified FT also in the continuous case, this symmetry does not hold for smaller values of $|u|$ even approximately. The reason why the modified FT holds approximately for the discrete systems considered in section 3 lies in the small number of states and therefore small number of paths with non vanishing winding number in both directions. As the number of states increases in the continuous limit this argument no longer holds and it is therefore far easier to produce deviations from the modified FT.

We illustrate this kind of behavior by using the potential energy $V(\mathbf{x}) = V_0 \cos(x_1 + x_2)$. The resulting generating functions and rate function are shown in figure 7. The symmetric bounds on both functions are plotted as dashed lines. Interestingly, for this choice of interaction potential they become tight for the extreme values.

The comparison of the rate functions for different coupling strengths reveals that stronger interaction between the two degrees of freedom leads to a decrease of the mean traveled distance. If the interaction is strong enough the visible degree moves against the direction of its driving force. The asymptotic behavior, however, is not affected by the coupling.

For the antisymmetric part of the rate function shown in figure 8, the interaction even leads to negative slopes at the origin if the visible degree of freedom moves against its driving force, while the asymptotic slope reaches the same value independently of the coupling strength since it only depends on the driving of the visible degree of freedom.

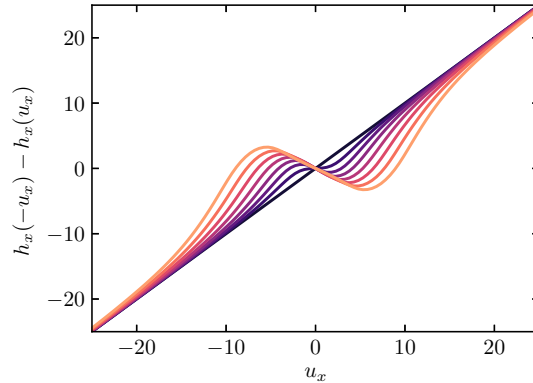


Figure 8. Antisymmetric part of the rate function for the parameter values shown in figure 7. If the hidden degree of freedom is not driven, the exact FT holds for the traveled distance of the observable colloid, since this quantity is in this case proportional to the total entropy production. If the hidden degree of freedom is driven, the FT holds only asymptotically for $|u_x| \rightarrow \infty$.

5.3. Reassessing the interpretation of the experimental data from [26]

So far, our analysis of the rate function has shown that a modified FT holds asymptotically for large observation times and large apparent entropy production. The experiments and simulations in [26], however, hinted at the validity of such a FT for finite times. The aim of this section is to put these findings in perspective.

First of all, one should keep in mind that the nature of the FT poses an inherent difficulty to experiments and, to lesser extent, also to simulations, since it states that events of negative apparent entropy production are exponentially suppressed. Therefore one needs to sample exponentially many events in order to expand the range in which the FT is tested. This range is typically limited to single digit multiples of k_B . The parameters used for the experiments in [26] were such that one rotation of the observable colloid produces several hundred k_B of apparent entropy; but since the antisymmetric part of the distribution can only be evaluated in a much smaller range, this means that the events entering in the modified FT reported in [26] are essentially only those for which the colloid is only moving a few degrees along the circumference of the ring in positive or negative direction.

Large deviation theory on the other hand describes the probability distribution in the limit of long observation times. As pointed out in [40], where a comparable system with hidden degrees of freedom has been analyzed, one can refine the results obtained from the rate function by also taking into account sub-exponential contributions to the distribution of an integrated current. These contributions introduce a fine-structured modulation of the probability distribution. The periodicity of the fine structure corresponds in the case of the two ring system to the amount of produced apparent entropy in one rotation.

For this reason, the experiments in [26] could only capture the fine-structure and

other subdominant transient contributions to the distribution. Likewise the simulation results for cases of broken FT presented therein are reminiscent of the impact of the fine-structure on the antisymmetric part of the distribution presented in [40]. Therefore, we can assume that the experiments only capture the leading order in $\Delta\tilde{s}_{\text{tot}}$ of the asymmetry of the probability distribution, which is in fact linear. The time-dependence of the slope of the modified FT in [26] can be explained by the transient contributions to the distribution.

6. Conclusion

We have generalized the notion of apparent entropy production introduced in [26] to arbitrary discrete networks and have shown that the extremes of the probability distribution of the apparent entropy production always obey a modified FT in the limit of long observation times. As demonstrated on the example of the bipartite lattice, this relation can be exploited to infer otherwise inaccessible properties, like in this case the true entropy \mathcal{A}_1 produced in one rotation of the visible degree of freedom, if the microscopic structure of the system is known.

The analysis of the bipartite lattice also shows that the modified FT is in some cases not restricted to the extremes of the distribution but holds approximately throughout the whole range of apparent entropy production. Even though this result resembles the experimental findings of [26], where a modified FT was observed for finite times, they are inherently different, since the argument explaining the modified FT for the bipartite grid is only applicable to a small number of states.

For a continuous state space, the modified FT holds only for the extreme fluctuations. As in the case of the bipartite lattice it is also possible to infer the true affinity of the observable degree of freedom from the slope of the modified FT. This slope, however, is not identical to the one observed for short observation times in experiments. It remains an open question whether it is possible to also infer information on hidden properties from the finite time modified FT.

Appendix A. Characteristic polynomial of the tilted operator

Our goal is to find a representation of the characteristic polynomial of the tilted Markov operator $\mathcal{L}(\lambda)$, that shows why the largest eigenvalue is approximately symmetric under the replacement $\lambda \rightarrow \lambda_0 - \lambda$.

The characteristic polynomial is defined as

$$\chi(\lambda, y) \equiv \det(\mathcal{L}(\lambda) - y) = \sum_{\pi \in S_{N^2}} \text{sgn}(\pi) \prod_n [\mathcal{L}_{n, \pi(n)}(\lambda) - y\delta_{n, \pi(n)}], \quad (\text{A.1})$$

where we used the Leibniz formula to express the determinant as a sum over all permutations π of the states. Each of these permutations can itself be expressed as a set of non overlapping cycles $\pi = \{\mathcal{C}_\pi^i\}$. Since the matrix $\mathcal{L}(\lambda)$ has only non-zero entries for connections that correspond to transitions with non-zero transitions rates,

all relevant cycles, i.e. those that lead to a non-zero term in the sum, are elements of the cycle space of the physical network that is studied. They can therefore be expressed as a superposition of the fundamental cycles \mathcal{C}_β of the network, i.e.

$$\mathcal{C}_\pi^i = \sum_{\beta} c_{\pi}^{i,\beta} \mathcal{C}_\beta. \quad (\text{A.2})$$

By identifying the diagonal part of the product in (A.1) as

$$\mathcal{D}_\pi(y) \equiv \prod_{n|\pi(n)=n} [r(n) - y], \quad (\text{A.3})$$

the product of all transition rates along the direction of the permutation as

$$\Gamma_\pi^+ \equiv \prod_{n|\pi(n) \neq n} w(n \rightarrow \pi(n)) \quad (\text{A.4})$$

and the sum of all increments of the integrated current along all cycles of the permutation as its effective affinity

$$\tilde{\mathcal{A}}_\pi \equiv \sum_{n|\pi(n) \neq n} d_{n,\pi(n)} = \sum_{n|\pi(n) \neq n} \ln \frac{\tilde{w}(n \rightarrow \pi(n))}{\tilde{w}(\pi(n) \rightarrow n)}, \quad (\text{A.5})$$

the characteristic polynomial simplifies to

$$\chi(\lambda, y) = \sum_{\pi \in S_{N^2}} \text{sgn}(\pi) \mathcal{D}_\pi(y) \Gamma_\pi^+ \exp(\lambda \tilde{\mathcal{A}}_\pi). \quad (\text{A.6})$$

Note that the diagonal part is the only quantity that depends on y .

To highlight the origin of the symmetry that is observed for the largest eigenvalue, we perform this sum twice and divide the result by two. The second sum runs over all inverse permutations π^{-1} . Obviously the diagonal does not change under this replacement and the product of rates along the cycles becomes the product of rates against the cycles

$$\Gamma_\pi^- \equiv \Gamma_{\pi^{-1}}^+ = \prod_{n|\pi(n) \neq n} w(\pi(n) \rightarrow n). \quad (\text{A.7})$$

This leaves us with

$$\chi(\lambda, y) = \sum_{\pi \in S_{N^2}} \text{sgn}(\pi) \mathcal{D}_\pi(y) \frac{1}{2} \left[\Gamma_\pi^+ \exp(\tilde{\mathcal{A}}_\pi \lambda) + \Gamma_\pi^- \exp(-\tilde{\mathcal{A}}_\pi \lambda) \right] \quad (\text{A.8})$$

$$= \sum_{\pi \in S_{N^2}} \text{sgn}(\pi) \mathcal{D}_\pi(y) \sqrt{\Gamma_\pi^+ \Gamma_\pi^-} \cosh \left(\tilde{\mathcal{A}}_\pi \lambda + \frac{1}{2} \mathcal{A}_\pi \right), \quad (\text{A.9})$$

where we introduced the true affinity of the permutation

$$\mathcal{A}_\pi \equiv \ln \frac{\Gamma_\pi^+}{\Gamma_\pi^-}. \quad (\text{A.10})$$

Since all cycles of the permutation can be decomposed into fundamental cycles the same is also true for the effective and actual affinity of the permutation, because those

are additive quantities. This allows us to write the argument of the hyperbolic cosine function in terms of the constants $c_\pi^{i,\beta}$

$$\chi(\lambda, y) = \sum_{\pi \in S_{N^2}} \text{sgn}(\pi) \mathcal{D}_\pi(y) \sqrt{\Gamma_\pi^+ \Gamma_\pi^-} \cosh \left[\sum_{c_\pi^i \in \pi} \sum_{\beta} c_\pi^{i,\beta} \left(\tilde{\mathcal{A}}_\beta \lambda + \frac{1}{2} \mathcal{A}_\beta \right) \right]. \quad (\text{A.11})$$

In this representation the fluctuation theorem for the total entropy production can be explained easily, since in this case all effective affinities of the fundamental cycles coincide with the actual affinities and the whole characteristic polynomial is therefore symmetric around $\lambda = -1/2$.

Since every term of the sum is for itself a symmetric function in λ , the whole characteristic polynomial can be approximately symmetric even if we do not consider the total entropy production, but if the effective affinities match the actual ones for sufficiently many fundamental cycles.

In the special case of the bipartite lattice there are only three different possible combinations of \mathcal{A}_β and $\tilde{\mathcal{A}}_\beta$, so the sum inside the hyperbolic cosine function in (A.11) reduces to

$$\chi(\lambda, y) = \sum_{\pi \in S_{N^2}} \text{sgn}(\pi) f_\pi(y) \cosh \left[\mathbf{n}_\pi \left(\tilde{\mathcal{A}} \lambda + \mathcal{A}_1/2 \right) + \mathbf{m}_\pi \mathcal{A}_2/2 \right], \quad (\text{A.12})$$

with $f_\pi(y) \equiv \sqrt{\Gamma_\pi^+ \Gamma_\pi^-} \mathcal{D}_\pi(y)$. The winding numbers \mathbf{n}_π and \mathbf{m}_π are the sums over the coefficients $c_\pi^{i,\beta}$ belonging to the visible or hidden fundamental cycles respectively, i.e.

$$\mathbf{n}_\pi = \sum_{c_\pi^i \in \pi} \sum_{\beta \text{ visible}} c_\pi^{i,\beta} \quad \text{and} \quad \mathbf{m}_\pi = \sum_{c_\pi^i \in \pi} \sum_{\beta \text{ hidden}} c_\pi^{i,\beta}. \quad (\text{A.13})$$

References

- [1] C. Jarzynski, “Equalities and inequalities: irreversibility and the second law of thermodynamics at the nanoscale”, *Annu. Rev. Condens. Matter Phys.* **2**, 329 (2011).
- [2] U. Seifert, “Stochastic thermodynamics, fluctuation theorems and molecular machines”, *Rep. Prog. Phys.* **75**, 126001 (2012).
- [3] C. Van den Broeck and M. Esposito, “Ensemble and trajectory thermodynamics: a brief introduction”, *Physica A* **418**, 6 (2015).
- [4] S. Rahav and C. Jarzynski, “Fluctuation relations and coarse-graining”, *J. Stat. Mech.* **2007**, P09012 (2007).
- [5] A. Gomez-Marín, J. M. R. Parrondo, and C. Van den Broeck, “Lower bounds on dissipation upon coarse graining”, *Phys. Rev. E* **78**, 011107 (2008).
- [6] A. Puglisi, S. Pigolotti, L. Rondoni, and A. Vulpiani, “Entropy production and coarse graining in Markov processes”, *J. Stat. Mech.* **2010**, P05015 (2010).
- [7] M. Esposito, “Stochastic thermodynamics under coarse graining”, *Phys. Rev. E* **85**, 041125 (2012).
- [8] B. Altaner and J. Vollmer, “Fluctuation-preserving coarse graining for biochemical systems”, *Phys. Rev. Lett.* **108**, 228101 (2012).
- [9] S. Bo and A. Celani, “Entropy production in stochastic systems with fast and slow time-scales”, *J. Stat. Phys.* **154**, 1325 (2014).
- [10] F. Knoch and T. Speck, “Cycle representatives for the coarse-graining of systems driven into a non-equilibrium steady state”, *New J. Phys.* **17**, 115004 (2015).

- [11] E. Zimmermann and U. Seifert, “Effective rates from thermodynamically consistent coarse-graining of models for molecular motors with probe particles”, *Phys. Rev. E* **91**, 022709 (2015).
- [12] M. F. Frenzel and T. Sagawa, “Coarse-grained hidden entropy production in partially inaccessible quantum jump trajectories”, *arXiv:1609.08628 [cond-mat, physics:quant-ph]* (2016).
- [13] É. Roldán and J. M. R. Parrondo, “Estimating dissipation from single stationary trajectories”, *Phys. Rev. Lett.* **105**, 150607 (2010).
- [14] M. Polettini and M. Esposito, “Effective thermodynamics for a marginal observer”, *Phys. Rev. Lett.* **119**, 240601 (2017).
- [15] N. Shiraishi and T. Sagawa, “Fluctuation theorem for partially masked nonequilibrium dynamics”, *Phys. Rev. E* **91**, 012130 (2015).
- [16] O. Flomenbom and R. J. Silbey, “Utilizing the information content in two-state trajectories”, *Proc. Natl. Acad. Sci. USA* **103**, 10907 (2006).
- [17] C. P. Amann, T. Schmiedl, and U. Seifert, “Communications: Can one identify nonequilibrium in a three-state system by analyzing two-state trajectories?”, *J. Chem. Phys.* **132**, 041102 (2010).
- [18] A. Alemany, M. Ribezzi-Crivellari, and F. Ritort, “From free energy measurements to thermodynamic inference in nonequilibrium small systems”, *New J. Phys.* **17**, 075009 (2015).
- [19] B. Bravi, M. Opper, and P. Sollich, “Inferring hidden states in langevin dynamics on large networks: average case performance”, *Phys. Rev. E* **95**, 012122 (2017).
- [20] P. Strasberg and M. Esposito, “Stochastic thermodynamics in the strong coupling regime: an unambiguous approach based on coarse graining”, *Phys. Rev. E* **95**, 062101 (2017).
- [21] U. Seifert, “First and second law of thermodynamics at strong coupling”, *Phys. Rev. Lett.* **116**, 020601 (2016).
- [22] C. Jarzynski, “Stochastic and macroscopic thermodynamics of strongly coupled systems”, *Phys. Rev. X* **7**, 011008 (2017).
- [23] A. Crisanti, A. Puglisi, and D. Villamaina, “Nonequilibrium and information: the role of cross correlations”, *Phys. Rev. E* **85**, 061127 (2012).
- [24] D. Gupta and S. Sabhapandit, “Fluctuation theorem for entropy production of a partial system in the weak-coupling limit”, *Europhys. Lett.* **115**, 60003 (2016).
- [25] J. Ehrich and A. Engel, “Stochastic thermodynamics of interacting degrees of freedom: fluctuation theorems for detached path probabilities”, *Phys. Rev. E* **96**, 042129 (2017).
- [26] J. Mehl, B. Lander, C. Bechinger, V. Blickle, and U. Seifert, “Role of hidden slow degrees of freedom in the fluctuation theorem”, *Phys. Rev. Lett.* **108**, 220601 (2012).
- [27] N. Uchida and R. Golestanian, “Generic conditions for hydrodynamic synchronization”, *Phys. Rev. Lett.* **106**, 058104 (2011).
- [28] J. Kotar, L. Debono, N. Bruot, S. Box, D. Phillips, S. Simpson, S. Hanna, and P. Cicuta, “Optimal hydrodynamic synchronization of colloidal rotors”, *Phys. Rev. Lett.* **111**, 228103 (2013).
- [29] Y. Izumida, H. Kori, and U. Seifert, “Energetics of synchronization in coupled oscillators rotating on circular trajectories”, *Phys. Rev. E* **94**, 052221 (2016).
- [30] J. Schnakenberg, “Network theory of microscopic and macroscopic behavior of master equation systems”, *Rev. Mod. Phys.* **48**, 571 (1976).
- [31] H. Touchette, “The large deviation approach to statistical mechanics”, *Phys. Rep.* **478**, 1 (2009).
- [32] P. Pietzonka, A. C. Barato, and U. Seifert, “Universal bounds on current fluctuations”, *Phys. Rev. E* **93**, 052145 (2016).
- [33] J. L. Lebowitz and H. Spohn, “A Gallavotti–Cohen-type symmetry in the large deviation functional for stochastic dynamics”, *J. Stat. Phys.* **95**, 333 (1999).
- [34] P. Tsoigni Nyawo and H. Touchette, “Large deviations of the current for driven periodic diffusions”, *Phys. Rev. E* **94**, 032101 (2016).
- [35] J. Mehl, T. Speck, and U. Seifert, “Large deviation function for entropy production in driven one-dimensional systems”, *Phys. Rev. E* **78**, 011123 (2008).
- [36] R. Chetrite and H. Touchette, “Nonequilibrium microcanonical and canonical ensembles and their equivalence”, *Phys. Rev. Lett.* **111**, 120601 (2013).

- [37] C. Maes and K. Netočný, “Canonical structure of dynamical fluctuations in mesoscopic nonequilibrium steady states”, *Europhys. Lett.* **82**, 30003 (2008).
- [38] A. C. Barato and R. Chetrite, “A formal view on level 2.5 large deviations and fluctuation relations”, *J. Stat. Phys.* **160**, 1154 (2015).
- [39] J. Hoppenau, D. Nickelsen, and A. Engel, “Level 2 and level 2.5 large deviation functionals for systems with and without detailed balance”, *New J. Phys.* **18**, 083010 (2016).
- [40] P. Pietzonka, E. Zimmermann, and U. Seifert, “Fine-structured large deviations and the fluctuation theorem: molecular motors and beyond”, *Europhys. Lett.* **107**, 20002 (2014).